Int. J. Electrochem. Sci., 9 **(2014)** 7152 - 7181

International Journal of
ELECTROCHEMICAL
SCIENCE
www.electrochemsci.org

Amperometric Gas detection: A Review

Linhongjia Xiong and Richard G. Compton[*]

Department of Chemistry, Physical and Theoretical Chemistry Laboratory, University of Oxford, South Parks Road, Oxford, United Kingdom OX1 3QZ.
[*]E-mail: richard.compton@chem.ox.ac.uk

Received: 23 July 2014 / *Accepted:* 5 September 2014 / *Published:* 29 September 2014

Recent progress in amperometric electrochemical gas sensing is reviewed. Topics covered include the use of room temperature ionic liquids (RTILs) as solvents in gas sensors, the advantageous use of micro-electrodes rather than macro-electrodes, membrane free devices and intelligent gas sensors including the simultaneous monitoring of temperature and humidity via voltammetric methods.

Keywords: Amperometric gas sensors, Clark Cell, Intelligent sensors, micro-electrodes, Room temperature ionic liquids.

1. INTRODUCTION

Gas detection plays an important, even essential role in many areas, ranging from food safety to environmental monitoring, with one of the best known examples being fire alarms based on CO[1-3] detection. Quantitative measurement of gases is based on a variety of physical or chemical principles[4]. Examples of commercialised sensors include techniques using spectrometry[5-9], luminescence[10-14] and electrochemistry[15-19] as a basis of sensing. Table 1 summaries different types of sensors and their operational principles. Amongst the various techniques, the electrochemical approach often shows significant advantages over the others. First and second, an electrochemical gas sensor provides high sensitivity at low cost. Third, their compact sizes allow for high portability. Fourth, only a small amount of energy is required to run the detector. On the other hand, the selectivity of electrochemical sensors is rarely perfect.

Electrochemical gas sensors are categorised as being either potentiometric or amperometric in nature. In the former, a potential, E, is established on a suitable electrode and related to the concentrations of the species giving rise to the potential via the concentrations of the Nernst equation[20]. Accordingly potentiometric sensors respond to the logarithm of the concentrations.

Figure 2 depicts the structure of one type of potentiometric gas sensing electrode. Note the presence of two reference electrodes and an internal solution.

Table 1. Table comparing of the principles of different gas sensing techniques. OV = organic vapour

Type	Principle	Some examples
Photoionization sensor	Detection of the charge generated from the ionised gas molecules produced by UV light	OV[4, 141-143], NO_2[144]
IR sensor	Comparison of IR intensity before and after being absorbed by the target gas	CO_2[145], CO[146], CH_4[147]
Fluorescence sensor[148]	Detection of the wavelength change of the fluorescence	CO[149],H_2S[150],HCN[151]
Metal oxide semiconductor	Measurement of changes in resistance after the gases absorbed on the semiconductor surface	H_2[152-154], NH_3[155, 156],NO_2[157], CO[158]
Catalytic gas sensor	Measure the resistance change on the sensor surface after reactions of target gas with the catalytic bead	OV[159], SO_2[160], CH_4[161, 162]
Electrochemical sensor	Detection of electron transferred during electrochemical reaction	O_2[63, 136, 163], NO_2[164], H_2S[165, 166], OV[164]

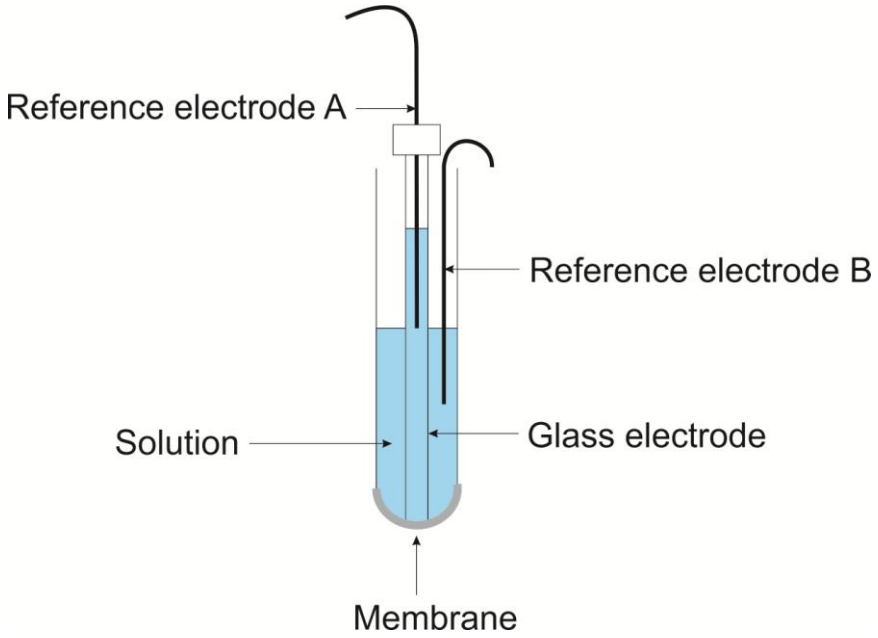

Figure 1. A potentiometric gas sensor electrode. The concentration of gas is recorded as the shift of potential. Gases, like CO_2, first diffuse through the membrane then dissolve in the internal solution. The pH of the solution is changed due to the formation of acidic compounds, like H_2CO_3. A potential shift of 59 mV with every one unit of pH is predicted by the Nernst equation[175].

Figure 2. Electrochemical gas sensors produced by Honeywell Analytics (www.honeywell.com). A electrochemical cell consists of electrodes, membrane and insulate separators (to keep electrodes away from each other). A detector case has a complete electronic circuit which allows the gas concentration to be read. A data recorder can continuously record the gas concentrations.

Gases like carbon dioxide [21-26], sulphur dioxide[27, 28] and ammonia[29-31] are detected potentiometrically where the gas concentrations can be read as shifts in the measured potential. Often the gases are not measured directly but indirectly via their equilibration with protons in aqueous solution (as in Figure 2) to give concentration via pH measurements. Nonetheless, most gas sensors are amperometrically based where the concentrations of gas are monitored by current measurements with the latter arising from electrolysis (oxidation or reduction) of a target gas at a working electrode. Amperometric sensors mostly originate from the design of the 'Clark oxygen electrode'[32] developed first for medical experiments. The Clark type gas sensor has a history of over five decades. In the immediately following sections, the classic and modern Clark type sensors are reviewed along with their advantages and drawbacks in the practical gas detection. Subsequently we address recent advances in the area of amperometric gas sensing including the use of room temperature ionic liquids (RTILs) as solvents and micro-electrodes as detectors.

2. CLARK TYPE SENSORS

2.1 History of the Clark Oxygen Electrode

The Clark oxygen electrode made its first appearance in 1956. It was invented by Professor Leland Clark[32], often considered to be the 'father of biosensors', and was designed to measure the 'tension'(concentration) of oxygen in blood and tested first on dogs. The device supported the publication of another Clark invention, an oxygen generator for cardiac surgery[33].

The original design consisted of a power supply, a platinum cathode, a potassium chloride-calomel anode (which was later replaced with a silver wire) and a cellophane membrane. All the electrodes were placed inside a glass tube and were wrapped with cotton soaked with saline solutions. The cellophane membrane was used to separate the internal and external environment in order to avert the influence of red blood cells in the oxygen measurements. To realise the detection, oxygen first diffuses through the membrane and enters the internal solution. The reduction of oxygen then takes

place at the platinum cathode (see Equation 1) when the power supply applies a potential of 0.6 V (vs. anode) to the cathode.

$$O_2 + 2H^+ + 2e \rightarrow H_2O_2 \quad (1)$$

The current of the reduction of oxygen was recorded using a galvanometer. The measured current was proportional to the concentration of O_2. This linear dependence of current on the concentration of dissolved oxygen was first discovered by Heinrich L. Danneel[34] as long ago as the nineteenth century as part of a study on dissolved oxygen in Nernst's laboratory. Experiments were performed by applying -0.2 V vs. platinum at a platinum macro-electrode in a water solution containing dissolved oxygen. In experiments with blood the biosensor failed since the platinum was blocked by adsorbed blood cells[35].

Experiments were carried out by Clark to optimise experimental conditions such as temperature, cathode voltage and choice of membrane material[32]. The current reading was observed to increase with the temperature due to the fact that oxygen diffuses faster at higher temperatures. The optimised voltage was within the range of 0.6 to 0.8 V against the anode but 0.6 V was deliberately chosen to reduce blood clot formation *in vivo*. It was found that the response time was largely limited by the time taken for oxygen diffusion through the membrane reflecting both the diffusion coefficient and solubility of oxygen in the membrane as compared to the aqueous electrolyte of the sensor as well as their relative thickness. The best membrane materials in order to decrease the response times were identified. A collection of polymers was investigated, including cellophane[32], dialysis tubing, condom rubber, condom skin and polyethylene. The time taken to reach steady state reading decreased in the following order[32]: condom skin > condom rubber > polyethylene = dialysis tubing > cellophane. The best response time (~ 20 s) was seen with cellophane membranes. However, the cellophane membrane slowed the response time by half as compared to what was observed without using a membrane (~ 10 s)[32].

After the conditions were optimised, experiments for oxygen detection were carried out on blood both *in vitro* and *in vivo*. *In vivo* oxygen sensing was achieved through inserting the Clark type electrode into the aorta of a heparinised[i], Nembutalized[ii] dog. The oxygen responses were recorded by a galvanometer. The first experiment was performed under different levels of oxygen where readings[iii] on the galvanometer of 74 and 96 indicated partial pressure of O_2 of 95 mm Hg and 700 mm Hg respectively. This design was proved to accurately reflect the oxygen content. The sensing stability using the Clark type electrode was determined under a constant air supply (3 hours) where identical signals were observed throughout the experiment[32].

The development of the Clark type oxygen electrode is deemed to be the birth of at-point-of-care measurements. Clerk cells subsequently allowed applications in gaseous oxygen monitoring, direct blood oxygen measurements and much later even the development of early glucose sensors[23]. This great invention has inspired numerous scientists of later generations to develop other gas sensors using the Clark oxygen electrode as the basis. These are discussed in the next section.

2.2 Modern Clark Type Gas Sensors

Modern gas sensors are typically derived from the original design of the Clark type electrode where the gas of interest first passes through a suitable permeable membrane and then dissolves in an internal solution where the electrochemical reaction takes place. Despite the diverse designs for different target gases, Clark type gas sensors share some common features where at least two electrodes are required and a gas selective membrane is used to retain the solvents. This basic design is the one used by companies such as Honeywell, Draeger, Alphasense, etc. to produce gas sensors for the market today. The general form of commercialised gas sensors is shown in Figure 2. As can be seen in Figure 2, a gas sensor consists of a electrochemical cell that contains electrodes, membrane and insulating separators (to keep electrodes away from each other), a detector case, which gives digital readings of gas concentrations, and a data recorder, which exports the gas concentrations into a computer. A summary of some gases that can be detected electrochemically using sensors supplied by different companies is shown in Table 2.

Table 2. Table of available gas sensors from different sensing companies.(as at May 2014) CH = hydrocarbon compounds and HX = hydrogen halide**.**

	O_2	CO_2	CO	PH_3	CH	NH_3	H_2S	HCN	SO_2	ClO_2	HX	Halogens	NO	NO_2	O_3	OV	H_2O_2	H_2
https://www.honeywellanalytics.com/																		
Honeywell	√	√	√	√	√	√	√	√	√	√	√	√	√	√	√	√	√	√
http://www.alphasense.com/																		
Alphasense	√	√	√	√		√	√	√	√	√	√	√	√	√		√	√	√
http://www.casellasolutions.com/																		
Casella	√		√	√		√	√	√	√	√	√	√		√		√	√	√
http://www.alphasense.com/																		
Draeger	√		√	√		√	√	√		√	√	√		√	√	√	√	√
http://www.geotechuk.com/																		
Geotech	√			√		√	√	√	√	√		√		√		√	√	√
http://www.indsci.com/																		
Industrial Scientific	√		√	√		√	√	√	√	√	√	√		√		√	√	√
http://www.ionscience.com/																		
Ion Science Ltd	√		√				√											
http://www.magusintl.com/																		
Magus International	√		√				√											
http://www.MSAsafety.com																		
MSA	√		√	√		√	√	√	√	√		√					√	
http://www.castlegroup.co.uk/																		

Castle Group Ltd	√	√	√	√	√	√	√	√	√	√	√	√	
http://www.emersonprocess.com/													
Net Safety	√	√		√	√		√					√	

Some companies focus on independently manufacturing and developing gas sensors for a full range of applications. Others may specialise in health and safety or environmental monitoring. The products are divided into small portable devices for field work and larger fixed devices used, for example, in ships or in the laboratory. It is noted that the sensors normally experience a life time of around 2 years, limited mainly due to the failure of the membrane and/or loss of the solvent (see next section). More details of gas sensing products in different companies can be found in the websites of the corresponding companies given in Table 2.

The value of a gas sensor depends on four properties: selectivity, sensitivity, response time and sensor lifetime. Selectivity allows the detection of a specific gas as other gases are either filtered out physically or chemically. Sensitivity indicates the dependence of the measured current on the concentration of gas. Factors influencing the sensitivity are not restricted to the electrode but reflect the sensing environment. Response times are also of vital importance since the sensor needs to reflect promptly the changing gas concentrations. This is normally measured by the time taken to reach 90% of the steady state response(t_{90}).

The sensor lifespan is controlled by the electrode materials, solutions and membranes. A sensor case (see Figure 2) lasts for a long time (> 100 years). An electrochemical sensor normally has a shelf life of 6 month to a year. In standard sensing environments (-40 to 50 ^{o}C, 20 - 90 % RH, ~ 1 atm)[36], the membrane lasts for ca. 3 years and the sensing probe can run more than several thousand detections.[iv] Lifetime limiting factors include the extreme temperature and pressures, low humidity environment and involvement of toxic gases[37]. These directly lead to consumed or contaminated filling solutions or electrode surfaces, resulting in electrode expiration.

2.3 Limitations

Despite the popular application of Clark type electrodes for gas detection, they suffer from some significant limitations. Lifespan, response time and sensitivity are greatly influenced by the use of membranes and conventional solvents as is next discussed.

One of the major drawbacks of Clark type electrodes in gas detection lies in the use of a membrane as the response time is largely limited by the time taken for diffusion through the membrane. It can be easily understood by comparing the diffusion coefficient of O_2 in air, water and in polymer membranes. The diffusion coefficient of O_2 in air [38] is 0.179 $cm^2\ s^{-1}$ (298 K) and in water [38] is 2.10×10^{-5} $cm^2\ s^{-1}$ (298 K) whereas in polymer membranes[39, 40] this value decreases to the order of magnitude of 10^{-6} $cm^2\ s^{-1}$. The decreased diffusion coefficient of oxygen in a membrane reflects the low gas permeability of polymer membranes[v]. In a typical Clark cell, the oxygen permeability in a membrane is 8×10^{-11} mol $m^{-1}\ s^{-1}\ atm^{-1}$ and in water is 2.7×10^{-9} mol $m^{-1}\ s^{-1}\ atm^{-1}$[41]. Note that the response time depends on both the membrane material and the thickness of the

membrane. The original work on the Clark electrode showed that the response time rose from 20 seconds to 30 seconds when the thickness of cellophane doubled. Table 3 summarises typical values of t_{90} for commonly detected gases using commercial sensors. Toxic gas sensors(H_2S, NH_3, SO_2 and NO_2) contain filling solutions of concentrated H_2SO_4 whilst that of O_2 sensors is an aqueous solution of potassium acetate[42]. The membrane is one type of gas permeable solid polymer membranes. Data collected from the user manuals of AlphaSense products show t_{90} of longer than 10 seconds. The prolonged response time due to the presence of the membrane makes some sensors impractical for real-time monitoring as the change of sensing conditions can happen within seconds or less. Membrane dependent sensitivity is another issue. For example, work by Do et al.[43] demonstrates that enhanced sensitivity was achieved by using conducting polymer membranes (polyaniline/Au/Nafion®) as working electrodes which not only reduces the need of a separate working electrode but also increases the sensitivity of nitrous oxide detection from 0.33 μA ppm^{-1}[44] to 2.28 μA ppm^{-1}.

Table 3. Table of t_{90} of some of the gases. Information is summaried from user's manuals of different gas sensing companies. Solutions for toxic gas sensor (H_2S, NH_3, SO_2, NO_2) sensor are concentrated H_2SO_4 and that of O_2 sensor is an aqueous solution of potassium acetate ($KC_2H_3O_2$). The membrane is one type of gas permeable solid polymer membranes.

Gas	t_{90}
O_2	< 11 s
NH_3	< 90 s
H_2S	< 15 s
SO_2	< 25 s
NO_2	< 25 s

Conventional solvents[45] used for gas detection are prone to evaporative losses, leading eventually to sensor failur[46]. Other sensing failures may be caused by high and low temperatures where solutions may be boiled or frozen in these environments. An electrochemical sensor normally has a lifetime of 24 month under standard conditions (~ 25 ^oC, ~ 60 % RH, and within 20 % of ambient pressure)[36].

H_2S, as an oil field gas, is one example that requires the sensor to be operated in extreme conditions (-60 to 60 ^oC)[47, 48] where shorter lifetimes may be expected. The internal solution electrolyte of commercial sensors is often composed of H_2SO_4/H_2O[49]as this electrolyte has a vapour pressure which most closely mirrors 'average ambient' conditions. However problems still remain as stated below. First the sensing range of the solution (-45 to 50 ^oC) is smaller than some real-world sensing conditions (-60 to 60 ^oC)[47]. Second losses of water result at humidity values lower than 60 % RH and gains of water at humidity values higher than this value. Experiments (by AlphaSense) in 5 M H_2SO_4 aqueous solution showed loss of the solution by ca. 50 % (by mass) at the temperature of 20 ^oC and at a humidity ranging from 0% to 25% RH over 2 days. At humidity values higher than 60 % RH, a 'flood' in the sensing chamber is caused where the solution increased by around 100% in mass, of water at the temperature of 20 ^oC and at a humidity of 95 % RH over 2 days.[vi] Such changes to the solvent compositions result in the need for constant calibration of sensors. Further to this, the narrow

electrochemical windows of H_2SO_4/H_2O (2 V) preclude useful electrochemical reactions of some gases to be observed in this media[50, 51].

Other limitations may be ascribed to the nature of the electrochemical process used analytically. Due to the electron transfer process involved in the gas detection, the diffusion coefficient, the number of electrons transfer and the gas concentrations are all sensitive to the environmental change. Therefore gas sensors typically are internally temperature and/or humidity compensated.[vii] This is discussed in later sections.

Cross sensitivity[viii] of non-target gases may result in a false reading of target gas concentrations. Taking an O_2 sensor as an example, an 6 % increase in signal is seen in the presence of 20 % CO_2. If more than 25 % CO_2 is present in the system, the O_2 sensor is damaged and an enhanced oxygen concentration is read, due to adsorption of CO_2 into the electrolyte($KC_2H_3O_2$).[xi] In addition, highly oxidising gases like chlorine, bromine, chlorine dioxide, and ozone can also interfere with oxygen sensing as electrons transferred during the oxygen reduction process can be possibly taken by those oxidising gases[42].

The next section focuses on overcoming some of the discussed limitations using recent advances.

3. ADVANCES

Recognising the limitations of the traditional Clark type oxygen sensors as discussed in the previous section, we next discuss recent developments aimed at overcoming these disadvantages. The following sections introduce recent advances for gas sensing systems from two respects: solvents and electrodes.

3.1 The use of ionic liquids for gas sensing

Room temperature ionic liquids (RTILs) are typically comprised of a bulky asymmetric organic cation and a small inorganic anion and exist as liquids at or below room temperature (298 K).[52] The main commercial suppliers of 'high purity' grade RTILs include Sigma-Aldrich[x], Merck[zi] and BASF[zii]. The purity of RTILs is frequently analysed[53] using electrochemical techniques[45, 52, 54], high-performance liquid chromatography[55-57], and X-ray photo-electron spectroscopy[58-60]. Figure 3 shows some commonly used ionic cations and anions. The contrasting sizes of the ions result in poor coordination and therefore at room temperature the materials are liquids rather than solids like NaCl. RTILs have special properties which can offer an alternative to conventional solvents for use in gas sensors. The following sections focus on the possible beneficial properties of RTILs and their applications in gas detection.

Wide Electrochemical Windows

The width of the electrochemical window of a system is determined by the oxidation and reduction potential of the supporting electrolytes or the solvents. Wider electrochemical windows allow a greater range of molecules to be detected without masking from background currents.

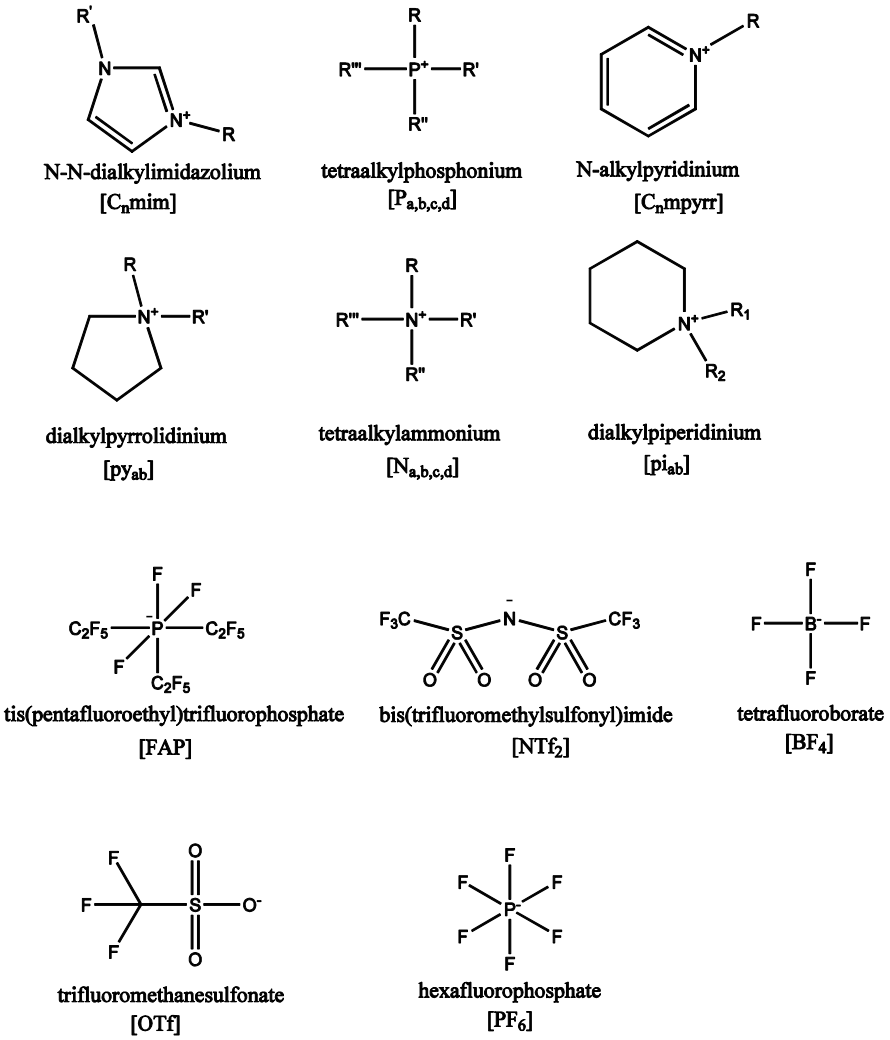

Figure 3. The structures, chemical names and usual abbreviations of the commonly used ionic components of RTILs

Water has an electrochemical window of 2.4 V and acetonitrile of 5 V. However, the oxidation or reduction potentials of the constituent ions are impossible to measure accurately. This is because the commonly used reference electrodes in RTILs are Ag or Pt pseudo reference electrodes which may cause potential drifts (around 5 mV). To overcome this issue, either a stable $Ag/AgNtf_2$ external reference electrode is made[61] or an internal reference probe, normally ferrocene(Fc) or ferrocene derivatives, is dissolved in RTILs. The latter is commonly adopted for simplicity. The electrochemical windows are defined as the potential corresponding to a current density[xiii] of 1 mA cm^{-2}. A low current density is deliberately chosen since only small current is used in gas detection[62-65]. A number of reports indicate that the oxidation and reduction potentials of ionic liquids are electrode material dependent[66-69]. The material dependence of electrochemical window was studied by Zhang and Bond[69] at Au, glassy carbon (GC) and Pt working electrodes in $[C_4mim][BF_4]$. The magnitude of the electrochemical reductive window adhered to the electrode material sequence of Au ≈ GC > Pt while the oxidation window magnitude followed the order Au > GC ≈ Pt.

O'Mahony et al. compared the cathodic and anodic limits of some frequently used ionic liquids. To collect these data, the potentials were measured against the Fc/Fc^+(ferrocene/ferrocenium) couple at 298 K and recorded at a Pt micro electrode. It was found that the anion followed the decreasing trend of stabilityO[47]: $[NTf_2] \approx [FAP] > [PF_6] \approx [BF_4] > [OTf] >$ halides (Br^-, I^-). As the counter ion may also influence the oxidation potential of the anion, the cations were fixed to be $[C_4mim]$ in this study. The cathodic limits decreased as: $[C_4mprr] \approx [P_{14,6,6,6}] \approx [N_{6,2,2,2}] \approx [C_6mim] > [C_4mim] \approx [C_4dmim] > [C_2mim]$. Here the anions were selected to be $[NTf_2]$ for fair comparison. The electrochemical windows of RTILs typically range from 3 - 6 V. The widest electrochemical window is reported to be $[N_{6,2,2,2}]$[FAP](7.0 V)[68, 70].

Table 4. Table of electrochemical window (EW) and conductivity (κ) of vacuum dried aprotic ionic liquids at, unless stated, 298 K. Data are collected and summaried from the literatures

ionic liquid	EW (V)[46]	κ($m\Omega^{-1}cm^{-1}$)[167]	thermal stability (K)	vapor pressure (Pa)
$[C_2mim][NTf_2]$	4.3	9.2[168]	455	0.0067
$[C_4mim][NTf_2]$	4.8	4.0[169]	450	0.0036
$[C_6mim][NTf_2]$	5	0.22[170]	428	0.012
$[C_6mim][FAP]$	5.3	0.17[171]	-	-
$[C_4mpyrr][NTf_2]$	5.2	2.1[167]	-	
$[C_4mim][OTf_2]$	4.9	2.9[172]	-	-
$[C_4mim][BF_4]$	4.7	0.36[170]	424	
$[N_{6,2,2,2}][NTf_2]$	5.4	0.67[173]		
$[P_{14,6,6,6}][NTf_2]$	5	-		
$[P_{14,6,6,6}][FAP]$	5.6	1.1 (Merck)	-	
water	2.4	13 [174][a]	2273	-
acetonitrile	5	7.6 [174][b]		

a. 0.1 M KCl as supporting eletrolyte.
b. 0.1 M TBAP as Supporting electrolyte, measured at 295 K.

Table 4 compares the electrochemical windows of some commonly used RTILs and the conventional solvents, water and acetonitrile[46].

Apart from the chemical nature of RTILs, other factors also have a large impact on the electrochemical window. The study by O'Mahony et al. showed[71] that the width of the electrochemical window is subject to both the water content and temperature. It was found that electrochemical window decreased in the following order of ionic liquid conditions: vacuum-dried > atmospheric > wet and 298 K > 318 K > 338 K. The temperature effect is because the electron transfer rate constant increases with the temperature. Hydrophobic RTILs may show less dependence on the width of electrochemical windows when exposed to atmospheric moisture as they uptake less water as compared to hydrophilic RTILs.[72] It was found by O'Mahony that the anion in particular affects the level of water uptake[47]. The hydrophobicity of the anions showed the following trend:[FAP] >

$[NTf_2]$ > $[PF_6]$ > $[BF_4]$ > halides. As for cations, long carbon chains enhance water repulsion in the solvent due to reduced polarity[73].

Inherent conductivity

Inherent conductivity is another important property of RTILs. It can be easily appreciated since RTILs are purely composed of ions. For RTILs, the extent of conductivity depends on the mobility of the ions composing the RTILs. The conductivity of RTILs near 298 K normally lies in the range of 0.12 - 8 $m\Omega^{-1}$ cm^{-1} which is comparable to organic solvents containing 0.1 M tetra-n-butylammonium perchlorate (TBAP) as supporting electrolyte where the values are within the range of 0.5 - 8 $m\Omega^{-1}$ cm^{-1}. Table 4 lists the conductivities of RTILs, water (0.1 M KCl as supporting electrolyte) and acetonitrile (0.1 M TBAP as supporting electrolyte).

The large range of conductivities of RTILs reflects their structural differences. Bulky constituent ions usually show slower movement. This is exemplified by comparing the conductivity of $[C_2mim][NTf_2]$, 9.2 $m\Omega^{-1}$ cm^{-1} and $[C_6mim][NTf_2]$, 0.22 $m\Omega^{-1}$ cm^{-1}. Here an order of magnitude drop is measured when the alkyl substituted group in the imidazolium changes from an ethyl to a hexyl group. Another cause of a decrease in mobility, hence conductivity, may be hydrogen bond formation[74]. The protic RTILs composed of fluoro- (F) or oxyl- (O) substituted anions generally show low conductivity ranging from 0.14 to 1.3 $m\Omega^{-1}$ cm^{-1}[69]. For the similar sized aprotic RTILs, the conductivities are above 4 $m\Omega^{-1}$ cm^{-1}, except [$[C_4mim][BF_4]$, where there may be some hydrogen bonds due to $[BF_4]$.

The conductivity can also be changed due to the external environment. Influential factors include temperature and the presence of additives. The variation of RTILs conductivity with temperature follows the Vogel-Tammann-Fulcher(VTF) relationship with an empirical equation[75] being

$$\kappa = AT^{-1/2}\exp\left[-B(T - T_0)\right] \quad (2)$$

From 258 K to 298 K, the conductivity of $[C_2mim][NTf_2]$ increases from 1.5 to 9.2 $m\Omega^{-1}$ cm^{-1}[76]. The higher conductivity at increased temperature reflects the increased mobility of the ions of RTILs. It was found that the addition of acetonitrile boosts the conductivity of imidazolium based RTILs where the conductivity of RTILs increases by more than 50 times with addition of just 15 % acetonitrile[77]. Similar observations were made with other co-solvents[78-81]. The use of organic co-solvent aims to decrease the solvent viscosity and hence increase conductivity.

Low Volatility

The volatility of a solvent is measured by its vapour pressure. The pressure is measured when the gas phase of the solvent is in equilibrium with its liquid phase. This property reflects the applicability of a solvent under extreme conditions, notably high temperature and low pressure. High vapour pressure indicates the likelihood of solvent losses under extreme environmental conditions. Compared to almost all conventional solvents, RTILs have much lower volatility. This is evidenced by its capability for use in X-ray Photo-electron Spectroscopy(XPS)[82]. XPS is generally not applicable

to liquids since it employs ultra-high vacuum (UHV) where conventional solvents evaporate. However XPS is now regularly used to characterise RTILs[83-88]. The vapour pressure of pure water[89, 90] at 298 K is 3167.73 Pa whereas that of most ionic liquids is few mPa at 298 K[91]. This significant difference reflects the much stronger inter-molecular (ionic) forces in RTILs.

High thermal stability

The suitability of RTILs as solvents in gas sensing depends on the range of possible operation temperatures which is defined mostly by the melting point and decomposition temperature. Note, however, that a RTIL may also evaporate below its decomposition temperature. Maton et al.[92] thoroughly reviewed the factors that may affect the thermal stabilities, decomposition mechanisms and tools to analyse thermal decomposition for many RTILs.

As compared to conventional solvents, RTILs often exhibit high thermal stability. This is evidenced by the fact that RTILs remain as liquids over a large temperature range. For example, $[C_4mim][NTf_2]$ is liquid between 184 and 723 K as compared to the range of 273 K to 373 K for water at 1 atm.

The high thermal stability of RTILs is ascribed to their stable component organic and inorganic ion structures. Decomposition of RTILs follows various mechanisms[93, 94], including nucleophilic substitution(S_{N1} and S_{N2})[95], thermal rearrangement[96], alkene formation and dealkylation[91].

RTILs containing halides experience relatively low thermal stability as halides are good nucleophiles and in IL media, strongly basic in nature. It is possible for halides to react with the cations, leading to alkyl chain cleavage, at temperatures as low as 373 K. The thermal stability of RTILs decreases with increasing nucleophilicity of the constituent anion.

Stable products resulting from decomposition encourage thermal decomposition at low temperatures[73, 97]. Long alkyl chains in the cation decreases thermal stability due to the favourable formation of stable carbon radicals. This is observed with basic anions, such as halides, $[PF_6]$, $[BF_4]$ and $[NTf_2]$. Because the conjugated radicals are stabilised through charge delocalisation, phenyl and allyl substituted cations show low thermal stability and decomposition via an S_{N1} mechanism may take place.

Tunability

Another advantageous feature of RTILs is their ‘tunability’. As RTILs consist of two ions, the composition of RTILs can be varied by altering either component and therefore they are frequently referred to as ‘designer solvents’. By simply modifying the composition of RTILs, the physical and chemical properties can ideally be tailored for particular needs. This is exemplified with work by Xiong et al.[98] where ferrocene oxidation potentials can be shifted by changing the size of the anion of the ionic liquids. Three anions were studied (in the order of increasing size): $[BF_4]$, $[NTf_2]$ and [FAP] with the same counter ion, $[C_4mim]$. Figure 3 shows the abbreviations. It was found that the oxidation potential of ferrocene increases with decreasing size of anion as presumably the ferrocenium cation is stabilised by with the presence of the smaller anion. This observation has the important implication that the oxidation potential of ferrocene, commonly used as an internal redox reference, can be tuned away from the potential of analytes of interest.

One method to tune the composition of RTILs is to simply mix two RTILs. This method has been used to optimise the solubility of CO_2 [99] and SO_2[100-102]. This variation in the concentration of the RTILs leads to different intermolecular interactions and hence to a change in the gas capture activity[100]. Binary mixtures of ionic liquids are not rare[103] as mixed RTILs commonly combine merits of the different components. A study by Fox et al.[104] shows that the conductivity of a mixture of $[py_{1,5}][NTf_2]$ and $[pi_{1,5}][NTf_2]$ (see Figure 3 for abbreviations) remains unchanged but the viscosity decreases as compared to the individual components.

Ionic liquids and gas sensors

In the context of their use in electrochemical gas sensors, RTILs are of particular interest as this can address some of the problem caused by conventional solvents[46]. A wide diversity of gas detection has been studied in RTILs. Rogers et al.[45] reviewed the reaction mechanisms of various gases, including O_2, CO_2, H_2, NH_3, H_2S, SO_2 and NO_2, in RTILs. Some electrochemical reactions in RTILs are shown in Table 5.

Table 5. Table of some electrochemical reactions of gas in RTILs[45].

Gas	Reaction in RTILs
O_2	$O_2 2 + e \longrightarrow O_2^-$
NH_3	$4NH_3 \longrightarrow 3NH_4^+ + 1/2N_{2(g)} + 3e$
H_2S	$H_2S + e \longrightarrow HS^- + H^\cdot$
SO_2	$SO_2 + e \longrightarrow SO_2^-$
NO_2	$NO_2 \longrightarrow NO_2^+ + e$

Examples of the use of RTILs for gas sensors include the application to CO_2 sensing where the wide voltammetric window allows the electrochemical reduction of CO_2 to be observed. Also RTILs are deemed good solvents for electrochemical H_2S sensors where a very wide range of temperature is typically required. The benefits of applying RTILs as solvents for gas sensors are next summarised.

First, the wider electrochemical windows provided by RTILs as compared to those seen in aqueous/organic system suggests that many more gases may be detected electrochemically by using RTILs in comparison to conventional solvents. Also the wider potential window allows different reactions to be studied.

Second with the use of RTILs as solvents, membrane free electrodes can be realised as proposed by Huang et al.[105] This advance arises because of the RTIL low or zero volatility[106] which prevents their significant evaporation. As discussed in Section 2.3, the use of membranes largely limits the response times. The use of membrane free RTILs potentially eliminates rate determining gas diffusion through the membranes thus possibly allowing much more rapid response times. Figure 4 shows a schematic design for a membrane free gas sensor.

Third, in contrast to conventional solvents that are likely to dry out or decompose at extreme temperatures or pressures(see Section 2.3), the low volatility and high thermal stability of RTILs allow

the sensors to function at extreme conditions (high/low temperature and pressures) without any losses in concentrations. This advantage not only ensures a longer lifetime of the gas sensors but also reduces the need of calibration.

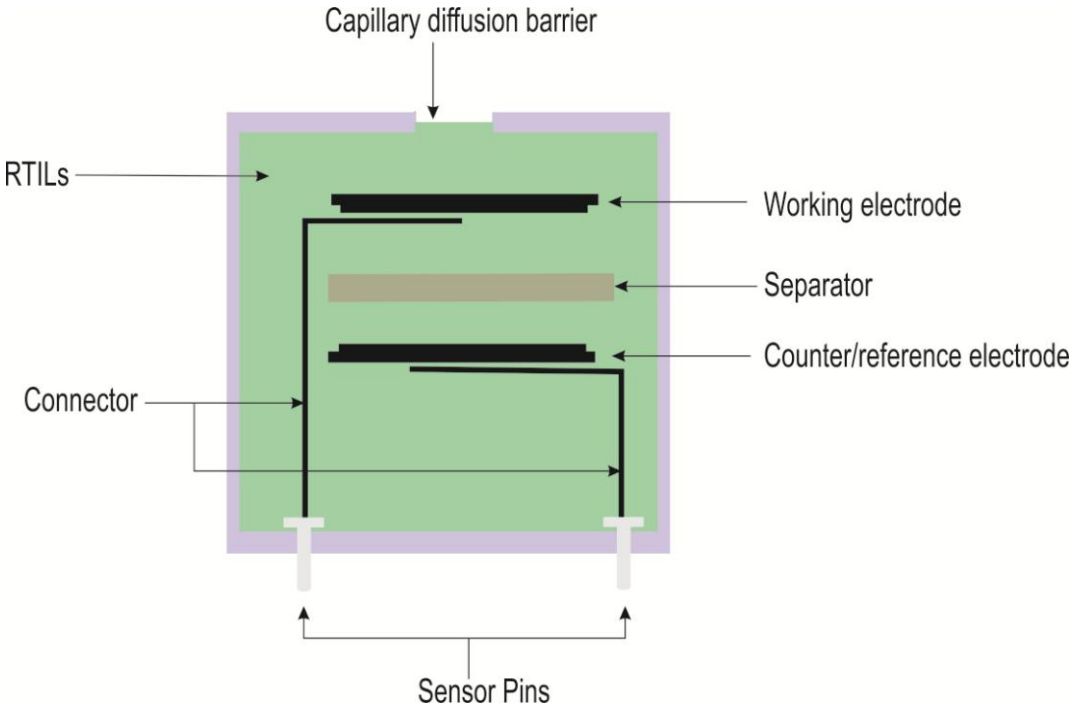

Figure 4. Proposed membrane-free gas detector

Fourth, RTILs are comprised of ions and hence they are fully supported solvents which reduce the need of additional supporting electrolytes. The ions composing RTIL can be tuned so as to enable RTIL to possess desired chemical and physical properties.

Fifth, RTILs are usually suggested to be used in three-electrode sensors, or if a working micro-electrode is used then a two-electrode system can be employed. The various reference electrodes for use in RTILs have been reviewed[45] and a Ag/Ag^+ electrode developed by Meng et al.[61]. However ferrocene and its derivatives are often used as internal redox references. Ferrocene itself has a significant volatility in RTILs solvents so analytes such as decamethylferrocene has been proposed. The tuneability of RTILs solvents has the benefit that the reference signal can be shifted away from the target analyte if necessary[107]. RTIL solvents often show ohmic resistances approximating to those seen for organic solvents in electrochemistry and as such are best studied using micro-electrodes as working electrodes. These are discussed in the next section.

3.2 The use of micro-electrodes for gas sensing

A micro-electrode is defined as having at least one dimension on the micro-scale (10 to 100 μm). Due to the relatively low conductivity and high viscosity of RTILs as compared to conventional solutions, micro-electrodes are widely employed to compensate these undesired features. This is

because micro-electrodes demonstrate higher mass transport rates, better signal-to-noise ratios and lower uncompensated resistances than macro-electrodes. These properties are detailed as below.

The diffusional regime (convergent or linear) is determined by the size of the electrode radius, r, relative to the diffusion layer thickness, (See equation 3)[20]. Within the experimental time scale (in the regime of r << d), convergent diffusion dominates at a micro-disc electrode as the electro-active materials are driven not only onto the electrode surface but also to the edge of the electrode[108]. A macro-electrode, on the other hand, experiences less effective linear diffusion (as r > d).

$$d = \sqrt{6Dt^{1/2}} \quad (3)$$

Here, D is the diffusion coefficient and t is the experimental time. Convergent diffusion dominates when r < d and linear diffusion occurs when r < d.

The use of micro-electrodes improves the signal-to-noise ratio since noise is proportional to the active electrode surface area whilst the signal depends on the total size of the diffusional field[20, 109]. A better signal-to-noise ratio leads a lower detection limit[42].

In addition, as less current is generated with a smaller electrode area, less solution resistance is experienced by a micro-electrode as compared to a macro-electrode in the same solution. Therefore a simple two-electrode system can be exploited by using a micro-electrode[20, 110].

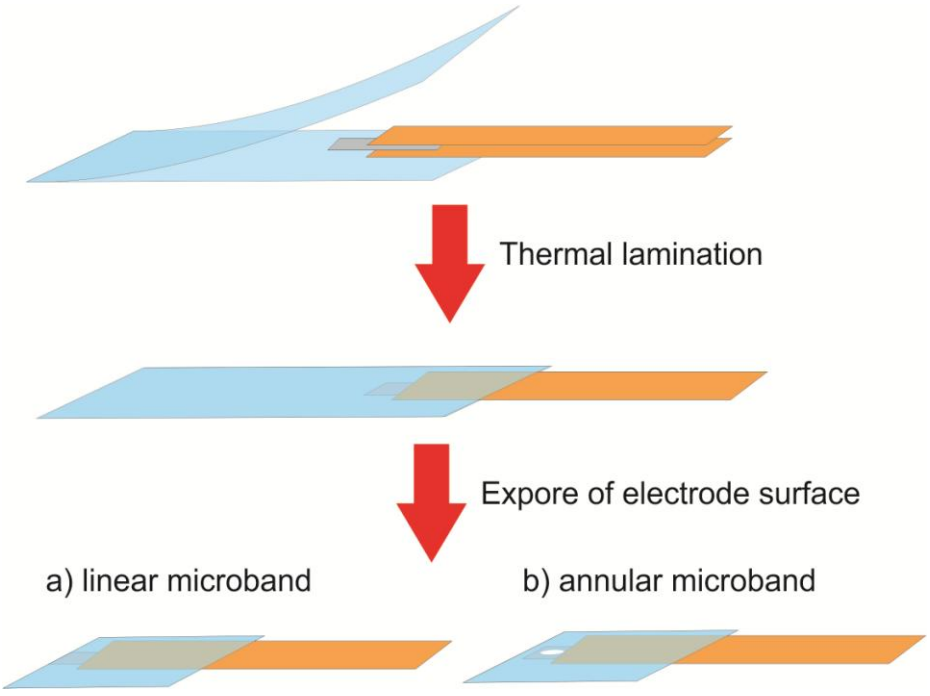

Figure 5. Fabraications of laminated a) platinum linear micro-band and b) platinum annular micro-band. Platinum foil is connected to a copper conductor and sandwiched between two pieces of laminating foil. The electrode is sealed by thermal lamination. A linear band is made by cutting the edge off (perpendicular to the lamination.) An annular band is made by punching a hole through the middle of the metal foil.

Xiong et al. have proposed a simple laminated method to produce both linear and annular band disposable micro-electrodes for oxygen detection[111, 112]. Figure 5 depicts the electrode fabrication methods where a piece of platinum was attached to a conducting material then was sandwiched between two pieces of laminating paper. The electrode was thermally sealed by a laminator. Micro-band electrodes were made either by cutting the edge off(linear band) or punching a hole through the middle(annular band). Proven by theory based upon diffusion onto band micro-electrodes[113], both electrodes demonstrated high capacity toward oxygen sensing with high reproducibility.

An array of micro-electrodes [105, 114] provides merit over a single micro-electrode as the use of large numbers of micro-electrodes operating in parallel not only enhances the sensing signals but also offers insurance against the failure of a few individual electrodes.

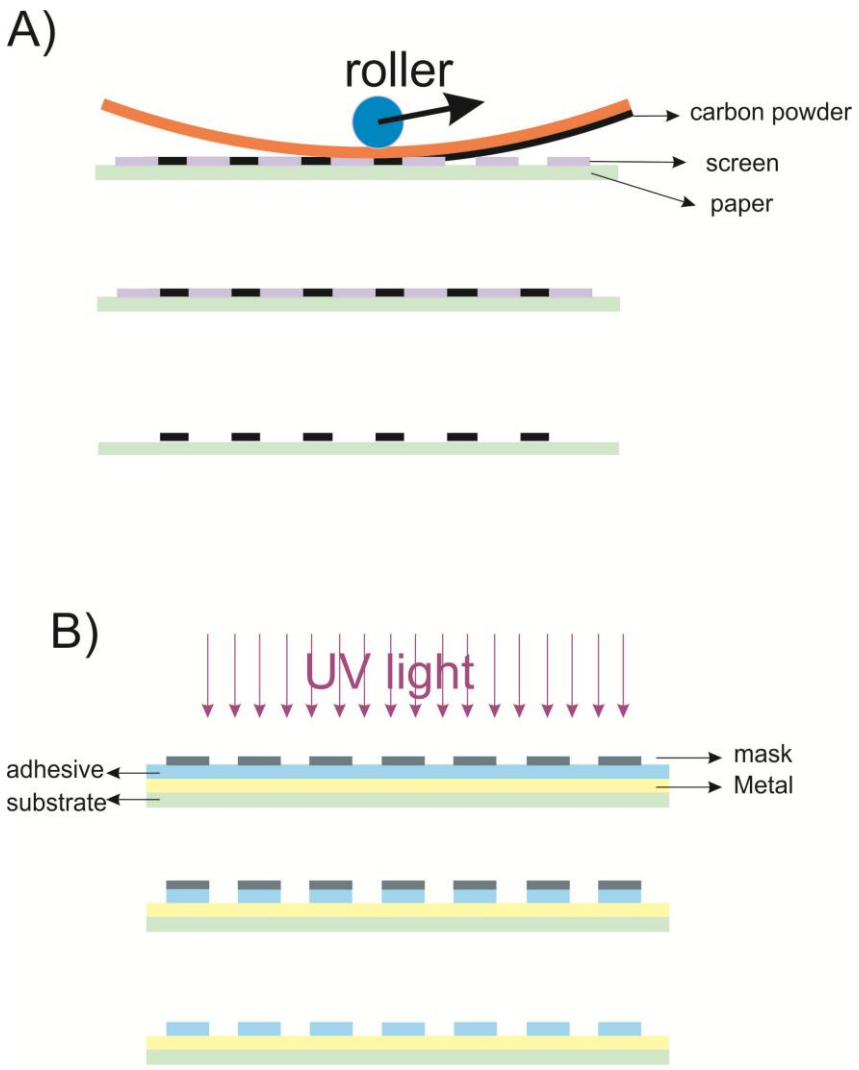

Figure 6. Schematic demonstrations of micro-electrode fabrications. a) Screen printed method. b) photo-lithography.

From the manufacturing aspect, disposable electrode arrays not only should be made of low-cost materials but also be feasible to be produced in bulk scale. Therefore, the manufacturing process

desirably avoids complex steps and uses accessible production equipment. Available fabrication methodologies including screen printing[115-118] and photo- or chemically etching[119-122]. Fabrication methods, along with the advantages and disadvantages of each method, have been extensively reviewed by Huang et al.[105]. Figures 6 a) and b) show two methods of micro-electrode array fabrication. Micro-electrode array suppliers include The Multi-Channel Systems[xiv], NanoFlex[xv], Micro Probe, Inc.[xvi] and AlphaOmega[xvii]. The choice of manufacturing method and electrode geometry dictate the usage and cost. Taking a 'well' electrode array as an example (see Figure 7), they are suitable for holding solvents inside the 3D well without the need of a separate cell. In order to test the validity of arrays of different geometries, such as micro-disc, micro-band and micro-pillar as shown in Figure 7, various mass transport models were developed to characterise the responses of these electrode arrays[123-125]. Benefiting from these available theories, micro-electrode arrays were used as working probes for gas detections[105, 126-128]. Griveau[126] has investigated the use of micro-disc arrays for amperometric NO monitoring which showed high selectivity and sensitivity. Further to this, simultaneous detection of NO and gases like CO_2 and O_2 has been developed.

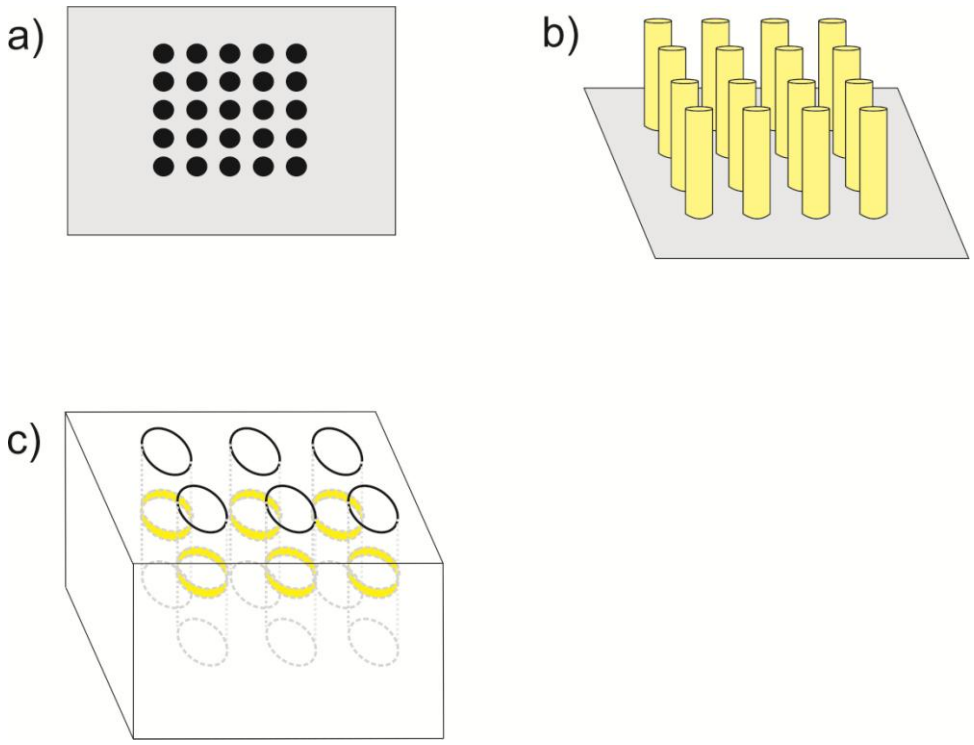

Figure 7. Different types of microarrays. a)A micro-disc electrode array. b)a micro-pillar electrode array. c) a micro-band array ('well' electrode array).

Huang et al.[105] successfully developed a membrane free oxygen sensor using micro-electrode arrays as working electrode and ionic liquids($[P_{14,6,6,6}][FAP]$) as solvents. This oxygen sensing system showed high sensitivity and most importantly, was freed from the problem caused by the use of membranes, especially frequent calibration.

4. INTELLIGENT GAS SENSORS

This section discusses recent achievement of designs towards intelligent sensors. Apart from providing accurate measurements of gas concentration, an intelligent sensor can also self-calibrate against changes of the sensing environment such as temperature and humidity.

The first part of this section is concerned with accurate measurements of gas concentrations by optimising chronoamperometry conditions. The second part focuses on the development of voltammetric temperature and humidity sensors to allow measurements 'at' the electrode surface rather than more remotely. The third part discusses the employment of a 'superoxide trapping' RTIL and its suitability in keeping an oxygen sensing system moisture insensitive.

4.1 Micro-disc electrode chronoamperometry: Shoup and Szabo analysis

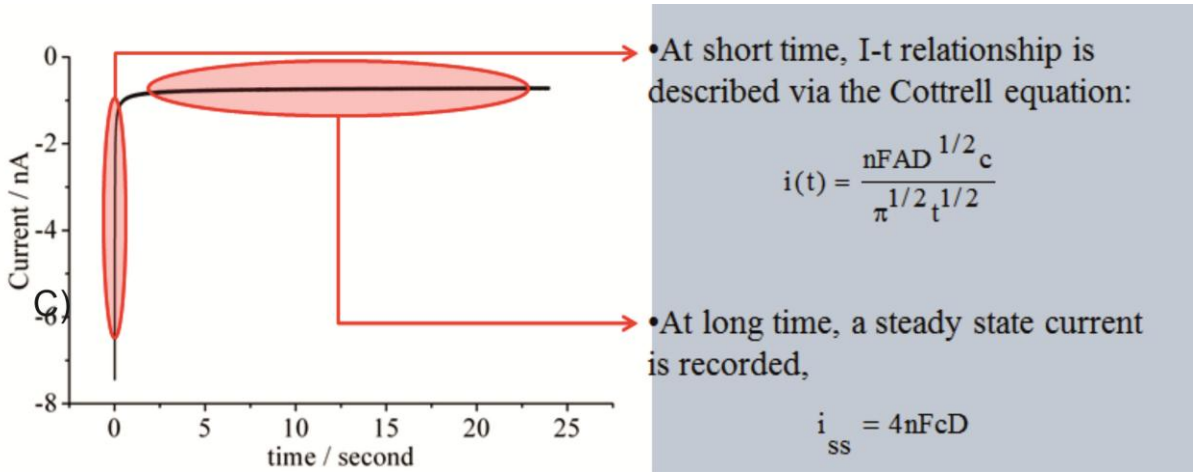

Figure 8. Demonstration of current responses at short time and long time.

Traditionally, the current generated by sensing (electrochemical) processes is used to reflect the concentrations of gas. However the current is not only dependent on concentration but also is a function of the number of electrons transferred during the electrochemical process and the diffusion coefficient of target molecules. An error in determining gas concentration may result from the change of any of these variables. This is not rare due to the fact that diffusion coefficients are sensitive to both temperature and humidity changes. Hence a method that allows simultaneous determination of concentrations and diffusion coefficients is advocated - specifically chronoamperometry has been used for this propose. In chronoamperometry, the potential steps from a potential where no current passes to a potential where the reaction of interest fully occurs in a diffusional controlled way. The current is record as a function of time. At the short time, the current response $i_{(t)}$ recorded at a planar disc electrode follows Cottrellian behaviour:

$$i_{(t)} = \frac{nFAD^{1/2}}{t^{1/2}\pi^{1/2}} \quad (4)$$

Here A is the electrode radius, D is the diffusion coefficient, c is the concentration of analyte, F is Faraday constant and t is the experimental time.

Whilst the current decays to zero for a macro-electrode, at longer time, a steady state current, i_{ss}, is seen at a micro-disc electrode:

$$i_{ss} = 4nFrDc \quad (5)$$

where r is the electrode radius and all other terms are defined as above. It is evident that at long time, current is a function of $ncD^{1/2}$ and at short time current is a product of ncD. Thus the parameters (nc) and D can be measured simultaneously through combining the current at short and long times.

Several models[129-132] have been proposed for simulating the current-time behaviour of chronoamperometry at micro-disc electrodes. Shoup and Szabo analysis is the most frequently used which describes chronoamperometric responses over all time values within an error of 0.5 %[131].

$$i = 4nFrDcf(t) \quad (6)$$

where

$$f(t) = 0.7854 + 0.8862\sqrt{\frac{r^2}{4Dt}} + 0.2146\exp\left(-0.7823\sqrt{\frac{r^2}{4Dt}}\right) \quad (7)$$

This equation is readily imported in data analysis software, such as Origin. Typically the value of electrode radius, r, is fixed as known and the software then automatically implements the fitting procedure. The values of c and D are iterated until the best fit (least difference between simulated and experimental current responses) is achieved.

Despite the simple operation of this technique, it was found by Xiong et al.[133] that values of concentration and diffusion coefficient of two systems (ferrocenes in acetonitrile and cobaltocenium in $[C_2mim][NTf_2]$) calculated by fitting Shoup and Szabo analysis to chronoamprometries for different transient times can vary slightly. This is because the Cottrellian current scales with $D^{1/2}c$ and the steady state current is a function of Dc (for n = 1). At too short measured times, capacitative non-Faradaic currents lead to large error whilst at long times the steady state signal dominates and many pairs of c and D gives same steady state current. Hence, accurate values of c and D are only possible when a 'good' balance between the Cottrellian current and the steady state current is measured.

In order to find out the optimised transient times, the simulated and experimental chronoamperometry at a range of transient times are compared to give the errors where the following equation is used:

$$\%\,\mathrm{MSAD} = \frac{1}{N}\sum_{N}\left|\frac{I_{\mathrm{sim}} - I_{\mathrm{exp}}}{I_{\mathrm{exp}}}\right| \times 100 \quad (8)$$

% MSAD is the mean scaled absolute deviation, I_{sim} is the simulated current and I_{exp} is the experimental current. MSAD corresponding to different pairs of c and D obtained from fitting simulations to experimental chronoamprometry of ferrocene oxidation at 1 s is shown in Figure 9. Through comparison of results obtained from Shoup and Shoup analysis and from MSAD evaluation, it was found that optimised transient time for the best value determinations depends on the

system(electrode size and analyte diffusion coefficient). Two examples in this work showed that the best transient time for ferrocene oxidation in acetonitrile is between 0.15 s and 0.5 s whereas cobaltocenium reduction in $[C_2mim][NTf_2]$ requires longer transient times (5 s).

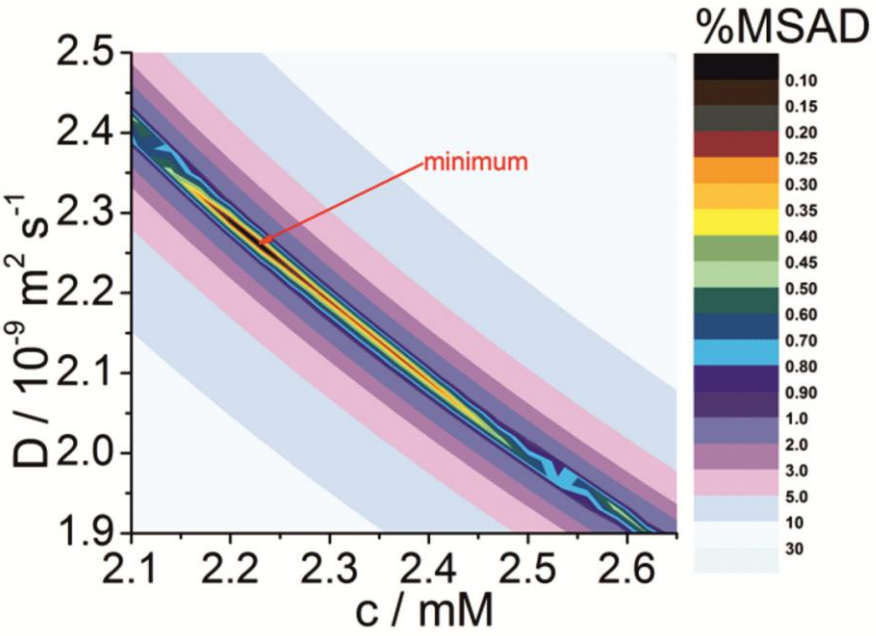

Figure 9. A 2D plot of MSAD. Colour listed on the right indicates the % MSAD. x axis is the concentraion and y axis is the diffusion coefficient of ferrocens. This plot is based upon the chronoamperometry of the ferrocene oxidation in acetonitrile. Reproduced by permission of tdhe Royal Society of Chemistry**.**

4.2 Temperature and Humidity

Since the values of nc and D can be achieved accurately using chronoamperometry along with Shoup and Szabo analysis, it is essential to consider other external factors on the sensing accuracy.

Due to the fact that an electrochemical gas sensor relies on the electron transfer process which is always highly sensitive to temperature and sometimes to humidity changes, the sensing accuracy is influenced by the change of environment. The affected parameters include the number of electron transfer, the concentration and the diffusion coefficient of solutes. How the environment plays part in these parameters is discussed below.

The following equilibrium is considered when a gaseous molecule is dissolved in a solution

$$A_{(g)} \rightleftharpoons A_{(dis)} \quad (9)$$

where $A_{(g)}$ is the analyte A in gas phase and $A_{(dis)}$ is dissolved A. Gas solubility and temperature normally exhibit a negative correlation[134] in ionic liquids as the equilibrium 9 shifts to the gaseous phase at higher temperature.

However this depends on the gases and solvents studied. CO_2 in $[C_4mim][Ac]$ is one of the exceptional cases, where a possible chemical step is involved during CO_2 dissolution[99, 135]. The correlation between dissolved gas concentrations and temperature are determined by the Van't Hoff equation.

$$\frac{\partial \ln K_{eq}}{\partial T} = \frac{\Delta H}{RT^2} \quad (10)$$

where K_{eq} is the equilibrium constant, ΔH is the standard enthalpy change and all other terms are defined as above.

The diffusion coefficient of a solute in ionic liquids generally increases with temperature. This correlation can often be predicted by the Arrhenius equation:

$$D = D_0 \exp\left(\frac{-E_a}{RT}\right) \quad (11)$$

Here, D is the diffusion coefficient and Ea is the energy of activation and all other terms are defined as before. The influence of humidity on the solubility is due to the solubility difference as water content of the ionic liquid changes. For example, for the pure solvents, the saturated solubility of oxygen in water is 1.2 mM and in $[P_{14,6,6,6}][Ntf_2]$ is 7.5 mM. The solubility of humidified oxygen in $[P_{14,6,6,6}][Ntf_2]$ ranges between these limits[136].

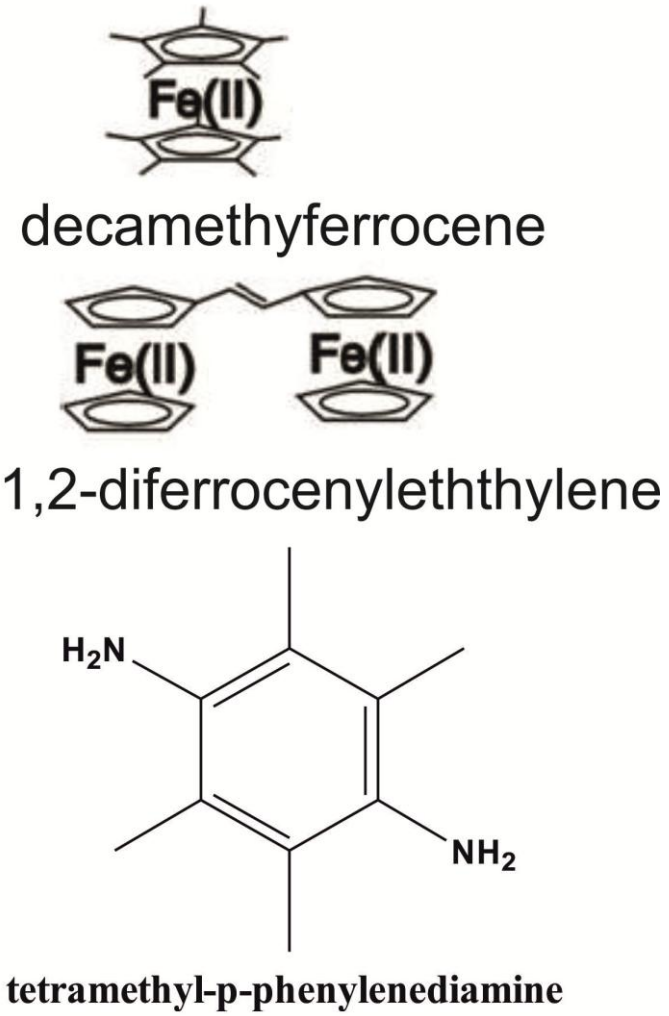

Figure 10. Molecular structures (from top to bottom) of decamethylferrocene, 1,2-diferrocenyleththylene and tetramethyl-p-phenylenediamine.

The diffusion coefficient of a gas is affected by change of humidity for similar reasons. Dissolved molecules are normally more mobile in water as compared to that in ionic liquids. Hence humidified oxygen shows a higher diffusion coefficient than dry oxygen in ionic liquids[136].

One solution to the problem caused by changed temperature and humidity is to keep the detection system under a restrictedly stable environment where the temperature is thermostatted and gases are pre-dried before experiment. However this is not realistic outside of the laboratory in sensor applications. A more practical approach is to measure the temperature and humidity of the sensing environment and correct the sensor measurements accordingly. An independent temperature and humidity sensor is potentially implantable in gas sensing systems for monitoring the change of experimental conditions. Commercially a solid state independent temperature and humidity sensor is used to measure the temperature and humidity in sensing solutions[137]. However an external probe may be remote from the sensing system, leading to a decreased sensitivity of temperature and humidity measurement.

Work by Xiong et al. proposed a built-in voltammetric temperature sensor incorporated into an amperometric oxygen sensor[138]. This voltammetric thermometer is able to measure the temperature at the electrode surface and therefore provides a real-time temperature. This thermometer is based on the potential difference in the formal potentials of two redox couples dissolved in the filling solutions of the sensor. The formal potential of a redox couple is related to the temperature according to the following equation:

$F\frac{\partial E_f^\circ}{\partial T} = \Delta S^\circ$	(12)

Here ΔS^o is the reaction entropy change. If two redox couples have different change of reaction entropy, the temperature dependency of formal potentials of these two redox couples varies. Therefore the *difference* of their formal potentials is a function of temperature. By employing a difference, absolute potentials are not needed so that constraints on the reference electrode are reduced.

Two suitable systems were chosen to be temperature indicators: a single molecule (1,2-diferrocenylethhthylene, see Figure 3 for molecular structure, in $[C_3mim][Ntf_2]$) and two independent molecules (decamethylferrocene and N,N,N′,N′-tetramethyl-p-phenylenediamine, see Figure 3 for molecular structures, in $[C_2mim][B(CN)_4]$) respectively. The temperature indicators were tested in both dry air and dry oxygen which indicated a high accuracy of temperature with an uncertainty smaller than ca. 1.5 K at 298 K without any influence on the oxygen detection.

After the success of the built-in voltammetric thermometer, a simultaneous temperature and humidity detector was developed by Xiong et al.[139]. The humidity sensor is based upon the observation made in Section 3.1 where the formal potential of a redox couple changes with the composition of ionic liquid. Therefore the differences of the ionic liquid composition due to different moisture levels can be indicated by the variation of the formal potential of a selected species.

To allow a simple measurement, the temperature sensor was humidity independent and vice versa. Ferrocene derivatives were chosen to measure both humidity and temperature due to their stability under extrame temperatures and pressures. Specifically decamethylferrocene (DmFc) and biferrocene(BiFc) were used. The potential difference between the oxidation of DmFc and the first oxidation of BiFc were found to be temperature independent. However the potential difference

between $DmFc/DmFc^+$ and $BiFc/BiFc^+$ are humidity dependent. On the other hand, the potential difference of $DmFc/DmFc^+$ and $BiFc^+/BiFc^{2+}$ shows temperature dependence with only slight humidity dependence. With this method, the temperature and humidity can be accurately measured and values of c and D at different humidity can be precisely determined and an iterative scheme to determine simultaneous values of temperature and humidity (See Figure 11).

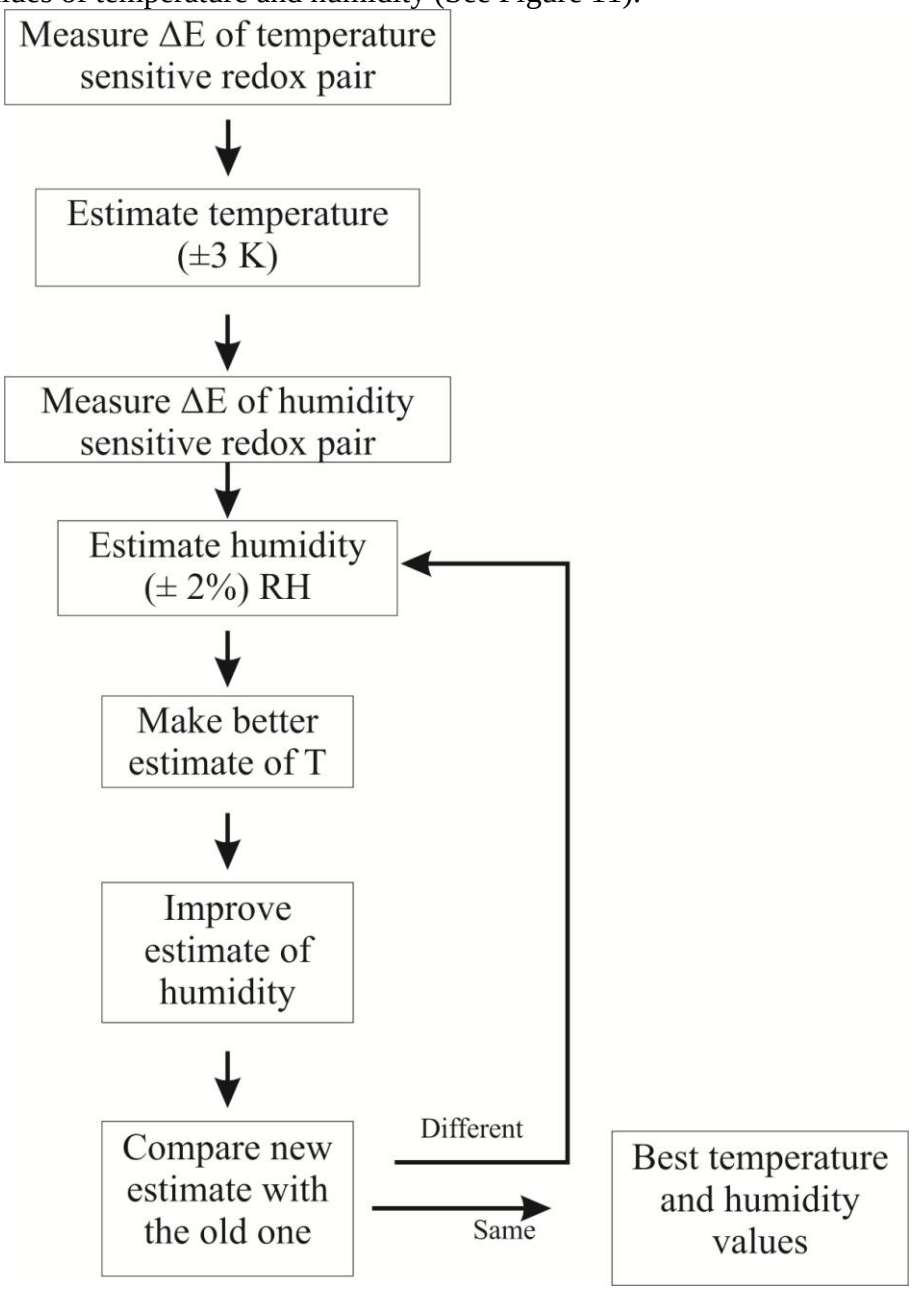

Figure 11. Scheme proposed to simultaneously determine the temperature and humidity.

4.3 Reactive ionic liquids

The reaction mechanism of dissolved molecules in ionic liquids may change with humidity. This is because dry protic ionic liquids are free from protons whereas water is a good source of protons. For example, the mechanism of dissolved oxygen (in ionic liquid) in the presence of moisture

can vary from 1 and 4 electrons transferred[62, 140]. Note that the number of electron transferred also depends on the electrode materials. The mechanism undergone at different humidity is unpredictable thus resulting in difficult and inaccurate measurements.

In particular the Shoup and Szabo micro-disc electrode analysis advocated above assumes that the number, n, of electrons transferred is known and constant. Then c and D are functions of humidity and temperature which can be calculated through the simultaneous humidity and temperature sensor. However this approach is not applicable for mechanisms involving a slow chemical step. Taking an ECE mechanism(see mechanism 13 to 15) as an example, the number of electrons determined by chronoamperometry can vary between 1 and 2 depending on the rate of reaction 14. This may be moisture sensitive and will certainly be temperature dependent.

$A + e \longrightarrow A^-$	(13)
$A^- \longrightarrow B$	(14)
$B \longrightarrow B^-$	(15)

An alternative approach, when coupled chemistry is involved, is to control the reaction at a known electron transfer stage. Work by Xiong et al. found a method to prevent the influence of water on the mechanism of oxygen reduction which is to 'trap superoxide' ions using phosphonium based ionic liquid. In dry RTILs the process is one electron but in the presence of water, H_2O_2 is formed in a two-electron reaction. Work by Evans et al. demonstrated the capability of phosphonium cation in trapping superoxide, $O_2^{\cdot-}$, and the following reaction was proposed.

$PR_4^+ + O_2^{\cdot-} \rightleftharpoons HO_2^{\cdot} + ylide$	(16)

Superoxide preferentially reacts with phosphonium cations to form ylide than with water. Therefore the oxygen reduction can be forced to stop at one electron transfer stage. Experiments carried out by Xiong et al. [136], along with relevant theory, showed that during oxygen reduction in the humidified $[P_{14,6,6,6}][NTf_2]$ (2 % to 36 % RH), oxygen follows an EC mechanism with one electron transfer:

$O_2 + e \longrightarrow O_2^{\cdot-}$	(17)
$O_2^{\cdot-} + [P_{14,6,6,6}]^+ \longrightarrow X$	(18)
$X - e \longrightarrow$ product	(19)

The only variables in this system were the concentration and diffusion coefficient of oxygen which greatly simplifies the oxygen detection in the humid conditions.

5. PROSPECTIVES

The above discussion shows that amperometric gas sensing has moved a long way from the original work of Clark. The widespread availability of commercial amperometric gas sensors speaks for the extensive value of the approach. Recent advances including the use of ionic liquids and micro-

electrode promote the development of intelligent gas sensors which can measure the local temperature and humidity and give data for an increasing variety of target gases.

References

1. D. Gutmacher, C. Foelmli, W. Vollenweider, U. Hoefer and J. Wöllenstein, *Procedia Engineering*, 25 (2011) 1121
2. S. C. Srivastava, R. J. Jaiswal, S. Sinha, R. V. K. Singh and R. N. Das, *Journal of Mines, Metals and Fuels*, 35 (1987) 384.
3. A. K. Sinha, D. P. Rajwar and A. K. Ghosh, *Journal of Mines, Metals and Fuels*, 35 (1987) 365.
4. S. Barnes and L. T. Old, *Chem. Eng. Prog.*, 105 (2009) 51.
5. R. P. Arasaradnam, J. A. Covington, C. Harmston and C. U. Nwokolo, *Alimentary Pharmacology and Therapeutics*, 39 (2014) 780.
6. B. Buszewski, D. Grzywinski, T. Ligor, T. Stacewicz, Z. Bielecki and J. Wojtas, *Bioanalysis*, 5 (2013) 2287.
7. M. Biniecka and S. Caroli, *TrAC - Trends Anal. Chem.*, 30 (2011) 1756.
8. F. Angerosa, *Eur. J. Lipid Sci. Technol.*, 104 (2002) 639.
9. R. C. Dorresteijn, C. D. De Gooijer, J. Tramper and E. C. Beuvery, *Biotechnol. Bioeng.*, 43 (1994) 149.
10. O. S. Wolfbeis, *Anal. Chem.*, 74 (2002) 2663.
11. X. Lu and M. A. Winnik, *Chem. Mater.*, 13 (2001) 3449.
12. J. N. Demas, B. A. DeGraff and P. B. Coleman, *Anal. Chem.*, 71 (1999) 793A.
13. M. C. Cheung, K. Y. Yung, H. Xu, N. D. Kraut, K. Liu, V. P. Chodavarapu, A. N. Cartwright and F. V. Bright, *IEEE J. Select. Topics Quantum Electron.*, 18 (2012) 1147.
14. C.-S. Chu, Y.-L. Lo and T.-W. Sung, *Photonic Sensors*, 1 (2011) 234.
15. N. V. Rees and R. G. Compton, *Energy and Environmental Science*, 4 (2011) 403.
16. G. Korotcenkov, S. D. Han and J. R. Stetter, *Chem. Rev.* , 109 (2009) 1402.
17. M. A. Rahman, P. Kumar, D.-S. Park and Y.-B. Shim, *Sensors*, 8 (2008) 118.
18. J. R. Stetter and J. Li, *Chem. Rev.* , 108 (2008) 352.
19. R. Knake, P. Jacquinot, A. W. E. Hodgson and P. C. Hauser, *Anal. Chim. Acta*, 549 (2005) 1
20. R. G. Compton and C. E. Banks, *Understanding Voltammetry 2nd Edition*, Imperial College Press (2011).
21. M. Maj-Zurawska and A. Hulanicki, *Chem. Anal.*, 54 (2009) 1149.
22. X. Xie and E. Bakker, *Anal. Chem.*, 85 (2013) 1332.
23. J. W. Severinghaus and A. F. Bradley, *J. Appl. Physiol.*, 13 (1958) 515.
24. C. R. Caflisch and N. W. Carter, *Anal. Biochem.*, 60 (1974) 252.
25. W. J. Cai, *Anal. Chem.*, 69 (1997) 5052.
26. H. Beyenal, C. C. Davis and Z. Lewandowski, *Sens. Actuators, B: Chemical*, 97 (2004) 202.
27. M. D. Mowery, *Anal. Chem.*, 71 (1999) 201.
28. I. Ben Youssef, H. Alem, F. Sarry, O. Elmazria, R. Jimenez Rioboo, C. Arnal-Harault and A. Jonquires, *Sens. Actuators, B: Chemical*, 185 (2013) 309.
29. Y. M. Fraticelli and M. E. Meyerhoff, *Anal. Chem.*, 53 (1981) 992.
30. M. E. Meyerhoff, Y. M. Fraticelli, J. A. Greenberg, J. Rosen, S. J. Parks and W. N. Opdycke, *Clin. Chem.* , 28 (1982) 1973.
31. M. A. Arnold, *Anal. Chim. Acta*, 154 (1983) 33
32. L. C. Clark Jr., R. Wolk, D. Granger and Z. Talor, *J. Appl. Physiol.*, 6 (1953) 189.
33. L. C. Clark Jr., F. Gollan and V. B. Gupta, *Science*, 111 (1950) 85.
34. H. L. Danneel, *Zeitschrift Elektrochemie*, 4 (1897) 227.
35. J. W. Severinghaus and P. B. Astrup, *Journal of Clinical Monitoring*, 2 (1986) 125.

36. P. T. Moseley, J. O. W. Norris and D. E. Williams, *Techniques and mechanisms in gas sensing*, Adam Hilger (1991).
37. A. Goswami and R. Cooper, *Anaesthesia & Intensive Care Medicine*, 12 (2011) 568
38. E. L. Cussler, *Diffusion: Mass Transfer in Fluid Systems*, Cambridge University Press (1997).
39. N. T. S. Evans and T. H. Quinton, *Respiration Physiology*, 35 (1978) 89
40. A. T. Haug and R. E. White, *J. Electrochem. Soc.*, 147 (2000) 980.
41. C. E. W. Hahn, *Analyst*, 123 (1998) 57R.
42. J. Wang, *Analytical Electrochemistry*, Wiley (2006).
43. J. S. Do and W. B. Chang, *Sensors and Actuators B: Chemical*, 72 (2001) 101
44. J.-S. Do and R.-Y. Shieh, *Sensors and Actuators B: Chemical*, 37 (1996) 19
45. E. I. Rogers, A. M. O'Mahony, L. Aldous and R. G. Compton, Amperometric gas detection using room temperature ionic liquid solvents, in, p. 473 (2010).
46. L. E. Barrosse-Antle, A. M. Bond, R. G. Compton, A. M. O'Mahony, E. I. Rogers and D. S. Silvester, *Chemistry - An Asian Journal*, 5 (2010) 202.
47. A. M. O'Mahony and R. G. Compton, *Electroanalysis*, 22 (2010) 2313.
48. D. Koschel, J.-Y. Coxam and V. Majer, *Industrial and Engineering Chemistry Research*, 46 (2007) 1421.
49. D. S. Silvester and R. G. Compton, *Z. Phys. Chem.*, 220 (2006) 1247.
50. E. Najdeker and E. Bishop, *J. ElectroAnal. Chem.*, 41 (1973) 79.
51. N. Ramasubramanian, *J. ElectroAnal. Chem.*, 64 (1975) 21.
52. M. C. Buzzeo, R. G. Evans and R. G. Compton, *ChemPhysChem*, 5 (2004) 1106.
53. A. Stark, P. Behrend, O. Braun, A. Muller, J. Ranke, B. Ondruschka and B. Jastorff, *Green Chem.*, 10 (2008) 1152.
54. U. Schroder, J. D. Wadhawan, R. G. Compton, F. Marken, P. A. Z. Suarez, C. S. Consorti, R. F. De Souza and J. Dupont, *New J. Chem.*, 24 (2000) 1009.
55. P. Stepnowski, A. MÃ¼ller, P. Behrend, J. Ranke, J. Hoffmann and B. Jastorff, *J. Chromatogr. A*, 993 (2003) 173.
56. P. Stepnowski, J. Nichthauser, W. Mrozik and B. Buszewski, *Anal. Bioanal. Chem.*, 385 (2006) 1483.
57. G. Le Rouzo, C. Lamouroux, C. Bresson, A. Guichard, P. Moisy and G. Moutiers, *J. Chromatogr. A*, 1164 (2007) 139.
58. K.-S. Kim, S. Choi, D. Demberelnyamba, H. Lee, J. Oh, B.-B. Lee and S.-J. Mun, *Chem. Commun.* , 10 (2004) 828.
59. S. Forsyth, J. Golding, D. R. MacFarlane and M. Forsyth, *Electrochimica Acta*, 46 (2001) 1753.
60. H. Matsumoto, H. Kageyama and Y. Miyazaki, *Chem. Lett.* (2001) 182.
61. Y. Meng, L. Aldous, S. R. Belding and R. G. Compton, *Phys. Chem. Chem. Phys.*, 14 (2012) 5222.
62. M. C. Buzzeo, O. V. Klymenko, J. D. Wadhawan, C. Hardacre, K. R. Seddon and R. G. Compton, *J. Phys. Chem. A*, 107 (2003) 8872.
63. R. G. Evans, O. V. Klymenko, S. A. Saddoughi, C. Hardacre and R. G. Compton, *J. Phys. Chem. B*, 108 (2004) 7878.
64. X. J. Huang, E. I. Rogers, C. Hardacre and R. G. Compton, *J. Phys. Chem. B*, 113 (2009) 8953.
65. L. Xiong, C. Batchelor-McAuley, L. M. Goncalves, J. A. Rodrigues and R. G. Compton, *Biosens. Bioelectron.*, 26 (2011) 4198.
66. E. I. Rogers, B. Sljukic, C. Hardacre and R. G. Compton, *J. Chem. Eng. Data* , 54 (2009) 2049.
67. P. A. Z. Suarez, C. S. Consorti, R. F. De Souza, J. Dupont and R. S. Gonçalves, *J. Braz. Chem. Soc.*, 13 (2002) 106.
68. P. C. Howlett, E. I. Izgorodina, M. Forsyth and D. R. MacFarlane, *Z. Phys. Chem.*, 220 (2006) 1483.

69. C. Zhao, G. Burrell, A. A. J. Torriero, F. Separovic, N. F. Dunlop, D. R. MacFarlane and A. M. Bond, *J. Phys. Chem. B*, 112 (2008) 6923.
70. N. V. Ignat'ev, U. Welz-Biermann, A. Kucheryna, G. Bissky and H. Willner, *J. Fluorine Chem.*, 126 (2005) 1150.
71. A. M. O'Mahony, D. S. Silvester, L. Aldous, C. Hardacre and R. G. Compton, *J. Chem. Eng. Data* , 53 (2008) 2884.
72. M. C. Buzzeo, C. Hardacre and R. G. Compton, *ChemPhysChem*, 7 (2006) 176.
73. J. Clayden, N. Greeves and S. Warren, *Organic Chemistry, 2nd edition*, Oxford University Press (2012).
74. M. S. Miran, H. Kinoshita, T. Yasuda, M. A. B. H. Susan and M. Watanabe, *Chem. Commun.*, 47(2011) 12676.
75. D. R. McFarlane, J. Sun, J. Golding, P. Meakin and M. Forsyth, *Electrochimica Acta*, 45 (2000) 1271
76. C. Schreiner, S. Zugmann, R. Hartl and H. J. Gores, *J. Chem. Eng. Data*, 55 (2010) 1784.
77. V. V. Chaban, I. V. Voroshylova, O. N. Kalugin and O. V. Prezhdo, *J. Phys. Chem. B*, 116 (2012) 7719.
78. C. Wang, P. Yan, H. Xing, C. Jin and J.-X. Xiao, *J. Chem. Eng. Data*, 55 (2010) 1994.
79. B. D. Fitchett, T. N. Knepp and J. C. Conboy, *J. Electrochem. Soc.*, 151 (2004) E219.
80. M. Bešter-Rogač, J. Hunger, A. Stoppa and R. Buchner, *J. Chem. Eng. Data* , 55 (2010) 1799.
81. A. Stoppa, J. Hunger and R. Buchner, *J. Chem. Eng. Data* , 54 (2009) 472.
82. D. S. Silvester, T. L. Broder, L. Aldous, C. Hardacre, A. Crossley and R. G. Compton, *Analyst*, 132 (2007) 196.
83. S. Caporali, U. Bardi and A. Lavacchi, *J. Electron. Spectrosc. Relat. Phenom.* , 151 (2006) 4.
84. R. Fortunato, C. A. M. Afonso, J. Benavente, E. Rodriguez-Castellan and J. G. Crespo, *J. Membr. Sci.*, 256 (2005) 216.
85. J. M. Gottfried, F. Maier, J. Rossa, D. Gerhard, P. S. Schulz, P. Wasserscheid and H.-P. Steinrück, *Z. Phys. Chem.*, 220 (2006) 1439.
86. O. Höfft, S. Bahr, M. Himmerlich, S. Krischok, J. A. Schaefer and V. Kempter, *Langmuir*, 22 (2006) 7120.
87. E. F. Smith, I. J. Villar Garcia, D. Briggs and P. Licence, *Chem. Commun.* (2005) 5633.
88. E. F. Smith, F. J. M. Rutten, I. J. Villar-Garcia, D. Briggs and P. Licence, *Langmuir*, 22 (2006) 9386.
89. G. A. Tunnell, *World distribution of atmospheric water vapour pressure*, H.M. Stationery Office (1958).
90. A. N. Nesmeianov, *Vapor pressure of the chemical elements*, Elsevier Pub. Co. (1963).
91. A. Chowdhury and S. T. Thynell, *Thermochim. Acta* , 443 (2006) 159
92. C. Maton, N. De Vos and C. V. Stevens, *Chem. Soc. Rev.*, 42 (2013) 5963.
93. D. Pletcher, *A First Course in Electrode Processes*, Royal Society of Chemistry (2009).
94. P. H. Rieger, *Electrochemistry*, Springer Netherlands (1994).
95. B. K. M. Chan, N. Chang and M. R. Grimmett, *Aust. J. Chem.*, 9 (1977) 2005
96. Y. Dessiaterik, T. Baer and R. E. Miller, *J. Phys. Chem. A*, 110 (2006) 1500.
97. P. Atkins and J. De Paula, *Atkins' Physical Chemistry*, Macmillan Higher Education (2006).
98. L. Xiong, A. M. Fletcher, S. G. Davies, S. E. Norman, C. Hardacre and R. G. Compton, *Chem. Commun.*, 48 (2012) 5784.
99. P. Li, M. C. Henstridge, L. Xiong and R. G. Compton, *Electroanalysis*, 25 (2013) 2268.
100. G. Cui, W. Lin, F. Ding, X. Luo, X. He, H. Li and C. Wang, *Green Chemistry*, 16 (2014) 1211.
101. G. Cui, J. Zheng, X. Luo, W. Lin, F. Ding, H. Li and C. Wang, *Angew. Chem. Int. Ed.*, 52 (2013) 10620.
102. C. Wang, G. Cui, X. Luo, Y. Xu, H. Li and S. Dai, *J. Am. Chem. Soc.*, 133 (2011) 11916.

103.M. Brussel, M. Brehm, A. S. Pensado, F. Malberg, M. Ramzan, A. Stark and B. Kirchner, *Phys. Chem. Chem. Phys.*, 14 (2012) 13204.
104.E. T. Fox, E. Paillard, O. Borodin and W. A. Henderson, *J. Phys. Chem. C*, 117 (2013) 78.
105.X.-J. Huang, L. Aldous, A. M. O'Mahony, F. J. del Campo and R. G. Compton, *Anal. Chem.*, 82 (2010) 5238.
106.F. Faridbod, M. R. Mohammad Reza Ganjali, P. Norouzi, S. Riahi and H. Rashedi, *Application of Room Temperature Ionic Liquids in Electrochemical Sensors and Biosensors*, InTech (2011).
107.L. Xiong, C. Batchelor-Mcauley, K. R. Ward, C. Downing, R. S. Hartshorne, N. S. Lawrence and R. G. Compton, *J. Electroanal. Chem.*, 661 (2011) 144.
108.D. K. Cope and D. E. Tallman, *Journal of ElectroAnal. Chem. and Interfacial Electrochemistry*, 188 (1985) 21
109.S. G. Weber, *Anal. Chem.*, 61 (1989) 295.
110.A. J. Bard and L. R. Faulkner, *Electrochemical Methods: Fundamentals and Applications*, Wiley (2001).
111.L. Xiong, P. Goodrich, C. Hardacre and R. G. Compton, *Sens. Actuators, B: Chemical*, 188 (2013) 978.
112.L. Xiong, D. Lowinsohn, K. R. Ward and R. G. Compton, *Analyst*, 138 (2013) 5444.
113.E. O. Barnes, L. Xiong, K. R. Ward and R. G. Compton, *J. Electroanal. Chem.*, 701 (2013) 59
114.O. Ordeig, J. Del Campo, F. X. Munoz, C. E. Banks and R. G. Compton, *Electroanalysis*, 19 (2007) 1973.
115.A. C. M. S. Dias, S. L. R. Gomes-Filho, M. M. S. Silva and R. F. Dutra, *Biosens. Bioelectron.*, 44 (2013) 216.
116.P. Kanyong, R. M. Pemberton, S. K. Jackson and J. P. Hart, *Anal. Biochem.*, 435 (2013) 114.
117.N. Xuan Viet, M. Chikae, Y. Ukita, K. Maehashi, K. Matsumoto, E. Tamiya, P. Hung Viet and Y. Takamura, *Biosens. Bioelectron.*, 42 (2013) 592.
118.N. Thiyagarajan, J.-L. Chang, K. Senthilkumar and J.-M. Zen, *Electrochem. Commun.*, 38 (2014) 86.
119.R. Prehn, L. Abad, D. Sánchez-Molas, M. Duch, N. Sabaté, F. J. Del Campo, F. X. Muñoz and R. G. Compton, *J. Electroanal. Chem.*, 662 (2011) 361.
120.T.-J. Wang, C.-F. Huang, W.-S. Wang and P.-K. Wei, *IEEE J. Lightwave Technol.*, 22 (2004) 1764.
121.T. J. Davies, S. Ward-Jones, C. E. Banks, J. del Campo, R. Mas, F. X. Munoz and R. G. Compton, *J. Electroanal. Chem.*, 585 (2005) 51
122.H. Lee, H. Shin, Y. Jeong, J. Moon and M. Lee, *Appl. Phys. Lett.*, 95 (2009) p. 071104.
123.C. A. C. Sequeira and D. M. F. Santos, *Z. Phys. Chem.*, 224 (2010) 1297.
124.K. R. Ward, L. Xiong, N. S. Lawrence, R. S. Hartshorne and R. G. Compton, *J. Electroanal. Chem.*, 702 (2013) 15
125.P. Tomčík, *Sensors (Switzerland)*, 13 (2013) 13659.
126.S. Griveau and F. Bedioui, *Anal. Bioanal. Chem.*, 405 (2013) 3475.
127.R. Chen, Y. Li, K. Huo and P. K. Chu, *RSC Adv.*, 3 (2013) 18698.
128.P. M. George, J. Muthuswamy, J. Currie, N. V. Thakor and M. Paranjape, *Biomed. Microdevices*, 3 (2001) 307.
129.M. Fleischmann and S. Pons, *Journal of ElectroAnal. Chem.*, 250 (1988) 257.
130.O. V. Klymenko, R. G. Evans, C. Hardacre, I. B. Svir and R. G. Compton, *J. Electroanal. Chem.*, 571 (2004) 211.
131.D. Shoup and A. Szabo, *J. Electroanal. Chem. Interfacial. Electrochem.*, 140 (1982) 237
132.J. Heinze, *Journal of ElectroAnal. Chem.*, 124 (1981) 73.
133.L. Xiong, L. Aldous, M. C. Henstridge and R. G. Compton, *Analytical Methods*, 4 (2012) 371.
134.J. Moore, C. Stanitski and P. Jurs, *Principles of Chemistry: The Molecular Science*, Cengage Learning (2009).

135. J. Zhang, S. Zhang, K. Dong, Y. Zhang, Y. Shen and X. Lv, *Chemistry - A European Journal*, 12 (2006) 4021.
136. L. Xiong, E. O. Barnes and R. G. Compton, *Sens. Actuators, B: Chemical*, 200 (2014) 157.
137. J. Courbat, Y. B. Kim, D. Briand and N. F. De Rooij, *IEEE J. Select. Topics Quantum Electron.*, p. 1356 (2011).
138. L. Xiong, A. M. Fletcher, S. Ernst, S. G. Davies and R. G. Compton, *Analyst*, 137 (2012) 2567.
139. L. Xiong, A. M. Fletcher, S. G. Davies, S. E. Norman, C. Hardacre and R. G. Compton, *Analyst*, 137 (2012) 4951.
140. E. I. Rogers, X. J. Huang, E. J. F. Dickinson, C. Hardacre and R. G. Compton, *J. Phys. Chem. C*, 113 (2009) 17811.
141. M. Suresh, N. J. Vasa, V. Agarwal and J. Chandapillai, *Sens. Actuators, B: Chemical*, 195 (2014) 44.
142. H. Hori, S. Ishimatsu, Y. Fueta, M. Hinoue and T. Ishidao, *J. UOEH*, 34 (2013) 363.
143. C. Yin, S. Q. Liu, Y. Z. Li and X. Y. Chen, *Applied Mechanics and Materials*, 336-338 (2013) 244.
144. A. Chiorino, G. Ghiotti, F. Prinetto, M. C. Carotta, D. Gnani and G. Martinelli, *Sens. Actuators, B: Chemical*, 58 (1999) 338.
145. E. Golinelli, S. Musazzi, U. Perini and F. Barberis, *Lecture Notes in Electrical Engineering*, 268 (2014) 19.
146. L. Dong, W. Ma, L. Zhang, W. Yin and S. Jia, *Guangxue Xuebao/Acta Optica Sinica*, 34 (2014) in press.
147. J.-P. Qiao, J.-M. Qin, X.-Y. Yan and Z.-X. Zhang, *Journal of Optoelectronics Laser*, 25 (2014) 217.
148. C. Li and G. Shi, *J. Photochem. Photobiol. C: Photochemistry Reviews*, 19 (2014) 20.
149. B. Kitiyanan, W. E. Alvarez, J. H. Harwell and D. E. Resasco, *Chem. Phys. Lett.*, 317 (2000) 497.
150. Q. Zhu and R. C. Aller, *Mar. Chem.* , 157 (2013) 49.
151. R. Jackson, R. P. Oda, R. K. Bhandari, S. B. Mahon, M. Brenner, G. A. Rockwood and B. A. Logue, *Anal. Chem.*, 86 (2014) 1845.
152. K. Zakrzewska, *Thin Solid Films*, 391 (2001) 229.
153. K. Vijayalakshmi, A. Renitta and K. Karthick, *Ceram. Int.*, 40 (2014) 6171.
154. V. I. Gaman, Y. Y. Sevast'yanov, N. K. Maksimova, A. V. Almaev and N. S. Sergeichenko, *Russian Physics Journal* (2014) in press.
155. J. Y. Patil, D. Y. Nadargi, J. L. Gurav, I. S. Mulla and S. S. Suryavanshi, *Mater. Lett.*, 124 (2014) 144.
156. Q. Qi, P.-P. Wang, J. Zhao, L.-L. Feng, L.-J. Zhou, R.-F. Xuan, Y.-P. Liu and G.-D. Li, *Sens. Actuators, B: Chemical*, 194 (2014) 440.
157. S. Kaci, A. Keffous, S. Hakoum, M. Trari, O. Mansri and H. Menari, *Appl. Surf. Sci.* (2014) in press.
158. M. C. Carotta, A. Fioravanti, S. Gherardi, C. Malagu, M. Sacerdoti, G. Ghiotti and S. Morandi, *Sens. Actuators, B: Chemical*, 194 (2014) 195.
159. J. Gu, Y. Zhang, J. Jiang and S. Li, *Chinese Journal of Scientific Instrument*, 35 (2014) 350.
160. Z. Darmastuti, C. Bur, P. Möller, R. Rahlin, N. Lindqvist, M. Andersson, A. Schütze and A. L. Spetz, *Sens. Actuators, B: Chemical*, 194 (2014) 511.
161. A. Somov, A. Baranov and D. Spirjakin, *Sensors and Actuators A: Physical*, 210 (2014) 157
162. E. Karpova, S. Mironov, A. Suchkov, A. Karelin, E. E. Karpov and E. F. Karpov, *Sens. Actuators, B: Chemical*, 197 (2014) 358.
163. P. Husson-Borg, V. Majer and M. F. Costa Gomes, *J. Chem. Eng. Data* , 48 (2003) 480.
164. W.-C. Chen, Y.-L. Hsu, S. Venkatesan and J.-M. Zen, *Electroanalysis*, 26 (2014) 565.
165. N. S. Lawrence, J. Davis, F. Marken, L. Jiang, T. G. J. Jones, S. N. Davies and R. G. Compton, *Sens. Actuators, B: Chemical*, 69 (2000) 189.

166.N. S. Lawrence, L. Jiang, T. G. J. Jones and R. G. Compton, *Anal. Chem.*, 75 (2003) 2499.
167.M. C. Buzzeo, C. Hardacre and R. G. Compton, *Anal. Chem.*, 76 (2004) 4583.
168.N. Hui, H. MinQiang, M. QingQing, L. YuanHui, Y. DeZhong and H. BuXing, *SCIENCE CHINA Chemistry*, 55 (2012) 1509.
169.M. Vranes, S. Dozic, V. Djeric and S. Gadzuric, *J. Chem. Eng. Data*, 57 (2012) 1072.
170.J. Hunger, A. Stoppa, S. Schrödle, G. Hefter and R. Buchner, *ChemPhysChem*, 10 (2009) 723.
171.J.-G. Li, Y.-F. Hu, S. Ling and J.-Z. Zhang, *J. Chem. Eng. Data*, 56 (2011) 3068.
172.O. Zech, A. Stoppa, R. Buchner and W. Kunz, *J. Chem. Eng. Data*, 55 (2010) 1774.
173.J. Sun, M. Forsyth and D. R. MacFarlane, *J. Phys. Chem. B*, 102 (1998) 8858.
174.D. R. Lide, *CRC Handbook of Chemistry and Physics, 85th Edition*, Taylor & Francis (2004).
175.R. G. Compton and G. H. W. Sanders, *Electrode Potentials*, OUP Oxford (1996).